

Boswellia serrata Extracts Ameliorates Symptom of Irregularities in Articular Cartilage through Inhibition of Matrix Metalloproteinases Activation and Apoptosis in Monosodium-Iodoacetate-Induced Osteoarthritic Rat Models

Jinhak Kim¹, Sangwon Eun¹, Hyunmook Jung², Jaehwan Kim², and Jinkyung Kim³

¹R&D Division, Daehan Chemtech Co., Ltd., Seoul 01811, Korea

²COSMAX BIO Inc., Chungbuk 27159, Korea

³Department of Food Innovation and Health, Kyung Hee University, Gyeonggi 17104, Korea

ABSTRACT: The research examined the effects of *Boswellia serrata* extracts (BSE) on a rat model of osteoarthritis induced by monosodium iodoacetate (MIA). The severity and progression of MIA-induced osteoarthritis were assessed using micro-computed tomography imaging. Additionally, the study investigated the impact of BSE various the biomarkers associated with osteoarthritis, including anabolic and catabolic factors, pro-inflammatory factors, and apoptosis factors. The evaluation methods employed included western blot, enzyme-linked immunosorbent assay, and real-time polymerase chain reaction analysis in osteoarthritic rats. Supplementing osteoarthritic rats with BSE reduced tissue injury, cartilage destruction, and decreased in MIA-induced roughness on the articular cartilage surface. MIA-treated rats exhibited increased expressions of phosphorylation of Smad3, MMPs, p-IκB, p-NF-κB, and pro-inflammatory factors (IL-1β, IL-6, TNF-α, and COX-2), which were mitigated by BSE supplementation. Furthermore, protein expressions related to apoptosis pathways were significantly reduced in MIA-induced rats supplemented with BSE. These findings suggested that BSE ingestion may enhance the inflammatory response, decrease JNK-dependent MMPs activation, and alleviate caspase-3-dependent apoptosis in MIA-induced osteoarthritic rat models. Consequently, BSE exhibits potential as a therapeutic agent for treating osteoarthritis.

Keywords: *Boswellia serrata*, matrix metalloproteinases, monosodium iodoacetate, osteoarthritis

INTRODUCTION

Osteoarthritis is a common condition among the elderly characterized by the gradual loss of articular cartilage in weight-bearing joints (Martin and Buckwalter, 2001; Kizawa et al., 2005). When these joints experience tissue injury, chondrocyte typically respond by enhancing proteoglycan and collagen synthesis. However, if this repair process fails, the articular cartilage can degenerate (Akkiraju and Nohe, 2015; Anderson and Johnstone, 2017). Arthritis occurs due to an imbalance between the destruction and synthesis of articular cartilage. The destruction of articular cartilage triggers the production of pro-inflammatory cytokines such as interleukin (IL)-1β, tumor necrosis factor (TNF)-α, and catabolic mediators like matrix metalloproteinase (MMP)-3, MMP-7, and MMP-13 (Grenier et al., 2014; Lu et al., 2015).

Osteoarthritis treatment aims to reduce pain reduction, delay disease progression, maintain functional status, and minimize cartilage damage. Typically, aerobic exercise is recommended along with interventions such as corticosteroids, acetaminophen, or nonsteroidal anti-inflammatory drugs (NSAIDs) to alleviate pain and inflammation, and inhibit disease progression (Sarzi-Puttini et al., 2005; Li et al., 2017). However, these medications can lead to severe side effects, including renal toxicity, gastrointestinal problems, vomiting, diarrhea, nausea, or an increased risk of cardiovascular complications (Hunter et al., 2011). Recently, there has been growing interest in complementary and alternative therapies, such as functional foods, nutraceuticals, and dietary supplements, to manage osteoarthritis and provide pain relief while delaying disease progression (Rosenbaum et al., 2010; Liu et al., 2018).

We analyzed the effects of *Boswellia serrata* extracts

Received 21 April 2023; Revised 23 May 2023; Accepted 23 May 2023; Published online 30 September 2023

Correspondence to Jinkyung Kim, E-mail: jkim2021@khu.ac.kr

© 2023 The Korean Society of Food Science and Nutrition.

© This is an Open Access article distributed under the terms of the Creative Commons Attribution Non-Commercial License (<http://creativecommons.org/licenses/by-nc/4.0>) which permits unrestricted non-commercial use, distribution, and reproduction in any medium, provided the original work is properly cited.

(BSE) on a rat model of osteoarthritis induced by monosodium iodoacetate (MIA). BSE is known in Indian Ayurveda for its medicinal properties against chronic inflammatory diseases contains terpenoids and boswellic acid, which are believed to possess anti-inflammatory and analgesic effects by targeting the 5-lipoxygenase and cyclooxygenase pathways. This inhibition reduces inflammatory mediators such as TNF- α and IL-6 (Siddiqui, 2011; Ammon, 2016). In this study, we investigated the impact of BSE on changes in joint structure, anabolic and catabolic factors, and inflammatory responses in a rat model of MIA-induced osteoarthritis.

MATERIALS AND METHODS

Preparation of the extract and reagents

BSE were provided by Daehan Chemtech Co., Ltd. and stored at -20°C until the experiment. The BSE sample was standardized based on the combined content of 3-acetyl-11-keto- β -boswellic acid and 11-keto- β -boswellic acid, with a 71 mg/g concentration. Reagents used for assessing the inflammatory response, anabolic and catabolic reactions of cartilage tissue, and apoptosis analysis were obtained from the following source: Rat IL-1 β , IL-6, and TNF- α duoset enzyme-linked immunosorbent assay (ELISA) kit from R&D Systems; HaltTM Protease and Phosphatase Inhibitor Cocktail from Thermo Fisher Scientific; complementary DNA (cDNA) synthesis kit and iQTM SYBR[®] Green Supermix from Bio-Rad Laboratories. The primer sequences are described in Table 1. Mini-PRETEAN[®] TGXTM Precast Gels, and Trans-Blot[®] TurboTM Transfer System were purchased from Bio-Rad Laboratories. Antibodies were obtained from Cell Signaling Technology or Abcam, and the details of the antibodies can be found in Table 2. All chemical reagents used were of high-performance liquid chromatography and molecular grade.

Table 1. Primer sequences for real-time polymerase chain reaction quantification of mRNA

Gene	Primer sequences
<i>Collagen type II</i>	F: 5'-GCA ACA GCA GGT TCA CGT ACA-3' R: 5'-TCG GTA CTC GAT GAT GGT CTT G-3'
<i>MMP-3</i>	F: 5'-GAG TGT GGA TTC TGC CAT TGA G-3' R: 5'-TTA CAG CCT CTC CTT CAG AGA-3'
<i>MMP-13</i>	F: 5'-TGA TGG GCC TTC TGG TCT TCT-3' R: 5'-CCC CGC CAA GGT TTG G-3'
<i>TIMP-1</i>	F: 5'-AAG GGC TAC CAG AGC GAT CA-3' R: 5'-ATC GAG ACC CCA AGG TAT TGC-3'
<i>TIMP-3</i>	F: 5'-GAC CGA CAT GCT TC CAA TTT C-3' R: 5'-GCT GCA GTA GCC ACC CTT CT-3'
<i>GAPDH</i>	F: 5'-TGG CCT CCA AGG AGT AAG AAA C-3' R: 5'-CAG CAA CTG AGG GCC TCT CT-3'

Animal treatment and MIA-induced osteoarthritis in rat

The experimental protocol was approved by the Institutional Animal Care and Use Committee of Kyung Hee University (KHGASP-22-252). Male Sprague-Dawley rats (6 weeks old) were obtained from Japan SLC, Inc. and housed under standard conditions (12 h light/dark cycle, 20~22 $^{\circ}\text{C}$, and 50~60% humidity). The rats were randomly divided into six groups, each consisting of six rats: a normal control group (NC) receiving a standard AIN 93G diet, a control group (C) with MIA injection and AIN 93G diet, a positive control group (PC) with MIA injection and AIN 93G diet methylsulfonylmethane (MSM) at a dose of 300 mg/kg body weight (BW), a BSE20 group with MIA injection and AIN 93G diet containing BSE at a dose of 20 mg/kg BW, a BSE50 group with MIA injection and AIN 93G diet containing BSE at a dose of 50 mg/kg BW, and a BSE100 group with MIA injection and AIN 93G diet containing BSE at a dose of 100 mg/kg BW. After 7 days of dietary administration, 50 μL (60 mg/mL) of MIA was injected into the knee joint. On day 31, the rats were sacrificed, and their knee joint tissues and serum were collected for analysis.

Microcomputed tomography (μCT) image scan

Formalin-fixed articular cartilage from rats was subjected to μCT imaging to assess the unevenness of the bone surface. The Skyscan 1172 X-ray μCT scanning system (Burker) was used for μCT image scanning. Scanned images were standardized, and data for each sample were collected using μCT software, ensuring consistent orientation.

Table 2. Antibodies used in the Western blot analysis

Biomarker	Host animal	Dilution for Western blot	Distributor
Smad3	Rabbit	1:1,000	CST
p-Smad3	Rabbit	1:1,000	CST
MMP-3	Rabbit	1:1,000	Abcam
MMP-13	Rabbit	1:1,000	Abcam
JNK	Rabbit	1:1,000	CST
p-JNK	Rabbit	1:1,000	CST
c-Fos	Rabbit	1:1,000	CST
p-c-Fos	Rabbit	1:1,000	CST
c-Jun	Rabbit	1:1,000	CST
p-c-Jun	Rabbit	1:1,000	CST
FADD	Rabbit	1:1,000	CST
Caspase 3	Rabbit	1:1,000	CST
Cleaved caspase 3	Rabbit	1:1,000	CST
Caspase 8	Rabbit	1:1,000	CST
Cleaved caspase 8	Rabbit	1:1,000	CST
β -Actin	Rabbit	1:1,000	LSbio

CST, Cell Signaling Technology; p-Smad3, phosphorylation of Smad3; MMP, matrix metalloproteinase; JNK, c-Jun N-terminal kinase; FADD, Fas-associated death domain protein.

Real-time polymerase chain reaction (PCR)

Total RNA was extracted from primary chondrocyte using the RNeasy extraction kit (QIAGEN) or chloroform (Sigma-Aldrich), following the manufacturer's instructions. cDNA synthesis from purified total RNA was performed using the iScript™ cDNA Synthesis kit. Real-time PCR was conducted using the CFX Connect™ Real-Time System (Bio-Rad Laboratories) with the iScript™ Green Supermix, cDNA, and custom-designed primers. Data analysis was performed using the CFX Maestro™ Analysis Software 3.1 (Bio-Rad Laboratories).

Western blot analysis

Total protein from cartilage tissue was dissolved in 4X NuPAGE LDS Sample Buffer (Life Technologies). Protein samples (100 µg protein from tissue) were separated by gel electrophoresis and transferred onto membranes. Subsequent processes including blocking, incubation with primary and secondary antibodies, visualization, and analysis, were conducted following previous methods (Kim et al., 2022).

Measurement of cytokines levels

The IL-1β, IL-6, and TNF-α levels were measured using an ELISA kit according to the manufacturer's instructions.

Statistical analysis

All data are presented as mean ± standard deviation. Differences among groups were evaluated using one-way analysis of variance and Duncan's multiple range test performed using IBM SPSS for Windows (ver. 23.0, IBM Corp.). Differences were considered significant at $P < 0.05$.

RESULTS AND DISCUSSION

Coronal µCT image and morphological analysis

Coronal µCT images of the hind knee joint showed that the MIA injection successfully induced degenerative osteoarthritis in control group compared to normal control group. However, treatment with BSE improved the damaged images of articular cartilage tissues. Morphological analysis of the trabecular bone beneath articular tissue revealed that BSE treatment resulted in significant increases in bone marrow density, bone volume ratio (BV/TV) and trabecular thickness (Tb.Th) at all doses. The trabecular number (Th.N) significantly increased only at the BSE100. While, BSE treatment resulted in significant decrease in the trabecular separation (Tb.Sp) at all doses. These results suggest that BSE supplementation may influence bone density and volume, but not on the number of trabeculae ($P < 0.05$; Fig. 1).

Measurement of anabolic and catabolic factors in cartilage tissue

The phosphorylation of Smad3, a protein involved in TGF-β signaling and the regulation of bone and cartilage growth, was measured. Treatment of MIA-induced osteoarthritis rats with BSE significantly increased the phosphorylation of Smad3 at the dose of BSE100 compared to the control group and BSE20 groups. This indicates that BSE may be crucial role in inhibiting the onset of MIA-induced osteoarthritis ($P < 0.05$; Fig. 2).

Anabolic and catabolic factors in cartilage tissue were also assessed. MMP-3 and MMP-13, enzymes responsible for cartilage, showed significantly restrained protein and mRNA expression in the BSE treatment groups compared to the control group. Additionally, the BSE treatment groups observed a clear dose-dependent reduction trend. On the other hand, BSE supplementation increased the mRNA expression of *collagen type II*, *TIMP-1*, and *TIMP-3* compared to the control group ($P < 0.05$; Fig. 3). These findings suggest that BSE may induce the anabolic pathway by activating Smad3 and suppress the catabolic pathway by inhibiting MMPs, thus contributing to the onset of degenerative osteoarthritis.

Inhibitory effect of BSE on the inflammatory response

Extensive research has shown that most inflammatory reactions are mediated by activating nuclear factor κB (NF-κB), composed of p65 and IκB. Most anti-inflammatory agents have targeted the suppression of NF-κB activation. NF-κB has been well established to be involved in the transcriptional activation of the COX-2 gene induced by IL-1β, TNF-α, and lipopolysaccharide (LPS) (Nakatani et al., 2004). The activation of the COX-2 gene in response to LPS has been demonstrated to be mediated by IκB kinase (IKK), which phosphorylates IκB, leading to its degradation and subsequent nuclear translocation of NF-κB. In macrophages, NF-κB, along with other transcription factors, coordinates the expression of genes related to the inflammatory process such as TNF-α, inducible nitric oxide synthase (iNOS), and COX-2 (Bonizzi and Karin, 2004).

BSE treatment significantly suppressed the phosphorylation of IκB, particularly at the dose of BSE100 group, suggesting the inhibition of NF-κB activation in the cytoplasm. This finding is further supported by the suppression of p65 phosphorylation in a dose-dependent manner. Consequently, the induction of COX-2 was inhibited similarly, sequentially related to a diminution in pro-inflammatory cytokines such as TNF-α, IL-1β, and IL-6 ($P < 0.05$; Fig. 4). These findings suggest that BSE may be involved, at least in part, in suppressing inflammation by inhibiting NF-κB activation in the early stage.

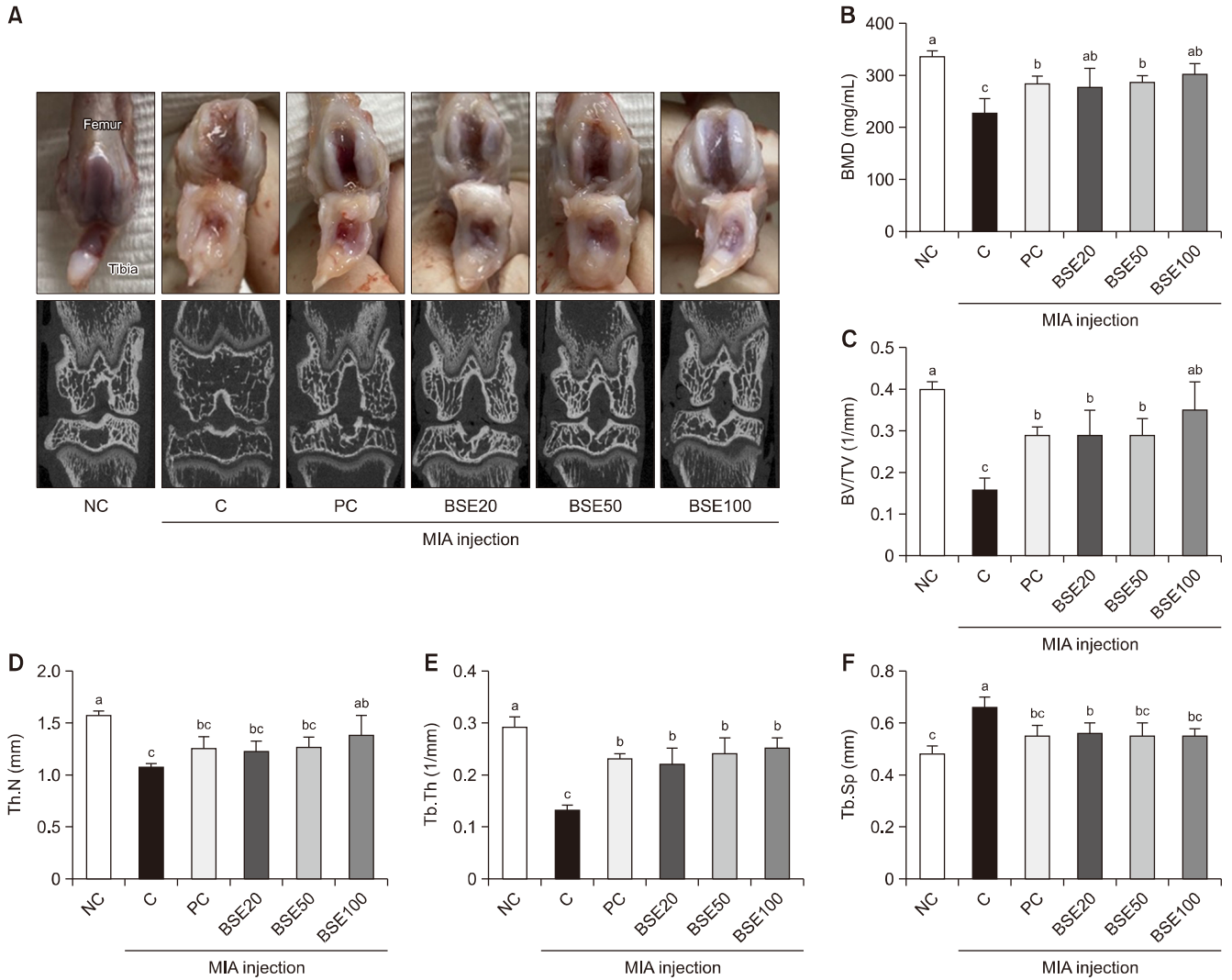


Fig. 1. The effect of *Boswellia serrata* extracts (BSE) on morphological change (A), bone marrow density (BMD, B), bone volume ratio (BV/TV, C), trabecular number (Th.N, D), trabecular thickness (Tb.Th, E), and trabecular separation (Tb.Sp, F) of rats with monosodium iodoacetate (MIA)-induced osteoarthritis using microcomputed tomography. Values are presented as mean±SD. Different letters (a-c) indicate a significant difference of $P<0.05$, as determined using Duncan’s multiple range test. NC, normal control group, AIN93G; C, control group, AIN93G+MIA injection; PC, positive control group, methylsulfonylmethane (MSM) 300 mg/kg body weight (BW) in AIN93G+MIA injection; BSE20, BSE 20 mg/kg BW in AIN93G+MIA injection; BSE50, BSE 50 mg/kg BW in AIN93G+MIA injection; BSE100, BSE 100 mg/kg BW in AIN93G+MIA injection.

The inhibition of BSE on cellular apoptosis in articular cartilage tissue

Apoptosis initiation is tightly regulated, and can be initiated through the intrinsic pathway (mitochondrial pathway) or the extrinsic pathway. The intrinsic pathway involves the release of cytochrome c from mitochondria, facilitated by the action of proteins Bax and Bak, which bind with apoptotic protease-activating factor-1 (Apaf-1) and activate caspase-9 and -3 as effectors. On the other hand, the extrinsic pathway is directly initiated by TNF and the Fas-Fas ligand interaction. The binding of TNF to its receptor (TNFR1 and TNFR2) triggers a pathway leading to caspase activation via TNF receptor-associated death domain (TRADD) and Fas-associated death domain protein (FADD), ultimately resulting in apoptosis (Wu and Bratton, 2013; Kashyap et al., 2021).

BSE treatment inhibited the caspase cascade pathway in this study compared to the control group, but there were no dose-dependent effects. In particular, caspase-8 and caspase-3 were significantly inhibited by BSE treatment. Additionally, pro-apoptotic factors FADD and Bax were significantly inhibited, although no dose-dependent effect was observed. BSE treatment also suppressed the phosphorylation of c-Jun N-terminal kinase (JNK), which in turn influenced the phosphorylation of c-Jun and c-Fos, inhibiting of cartilage cell destruction ($P<0.05$; Fig. 5).

In conclusion, BSE may ameliorate degenerative osteoarthritis, through multiple mechanisms. It appears to inhibit inflammation by inactivating NF-κB, blocking the caspase-3 pathway associated with FADD and Bax suppress cartilage cell apoptosis and inhibiting the phosphorylation of the JNK pathway from reducing the activation

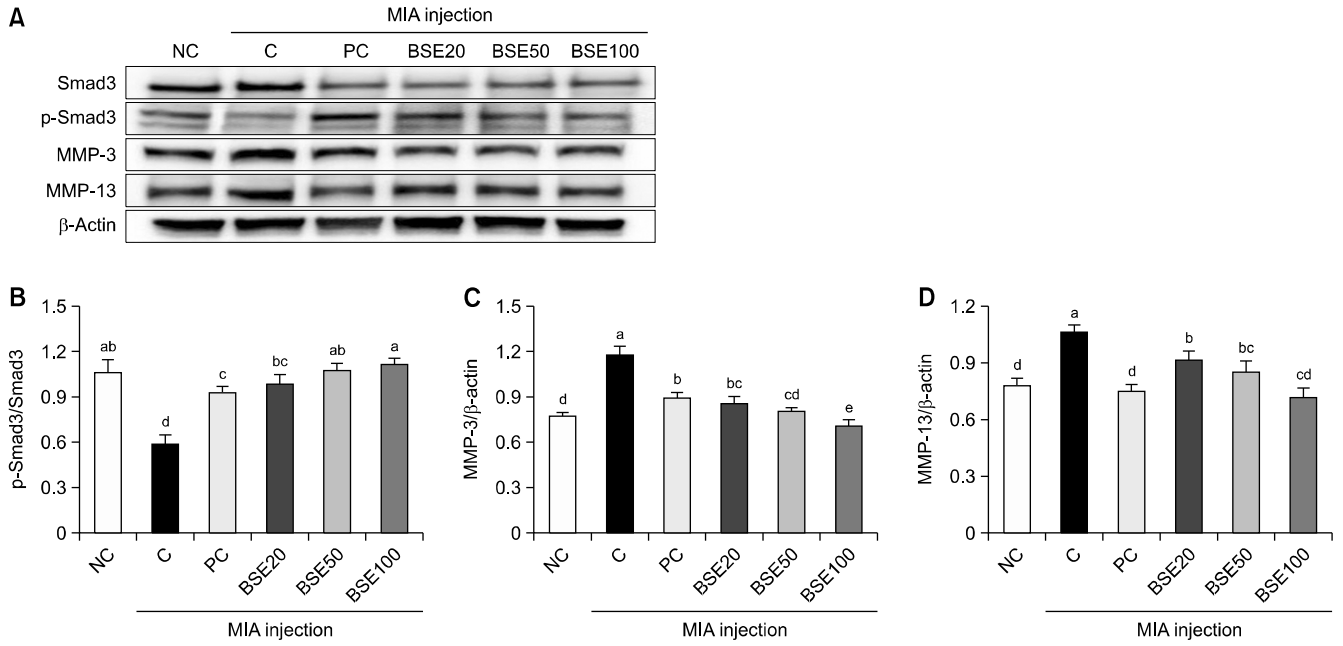


Fig. 2. The effect of *Boswellia serrata* extracts (BSE) on protein expressions of Smad3 (A, band image; B, quantification), matrix metalloproteinase (MMP)-3 (C), and MMP-13 (D) of rats with monosodium iodoacetate (MIA)-induced osteoarthritis. Values are presented as mean \pm SD. Different letters (a-d) indicate a significant difference of $P < 0.05$, as determined using Duncan's multiple range test. NC, normal control group, AIN93G; C, control group, AIN93G+MIA injection; PC, positive control group, methylsulfonyl-methane (MSM) 300 mg/kg body weight (BW) in AIN93G+MIA injection; BSE20, BSE 20 mg/kg BW in AIN93G+MIA injection; BSE50, BSE 50 mg/kg BW in AIN93G+MIA injection; BSE100, BSE 100 mg/kg BW in AIN93G+MIA injection; p-Smad3, phosphorylation of Smad3.

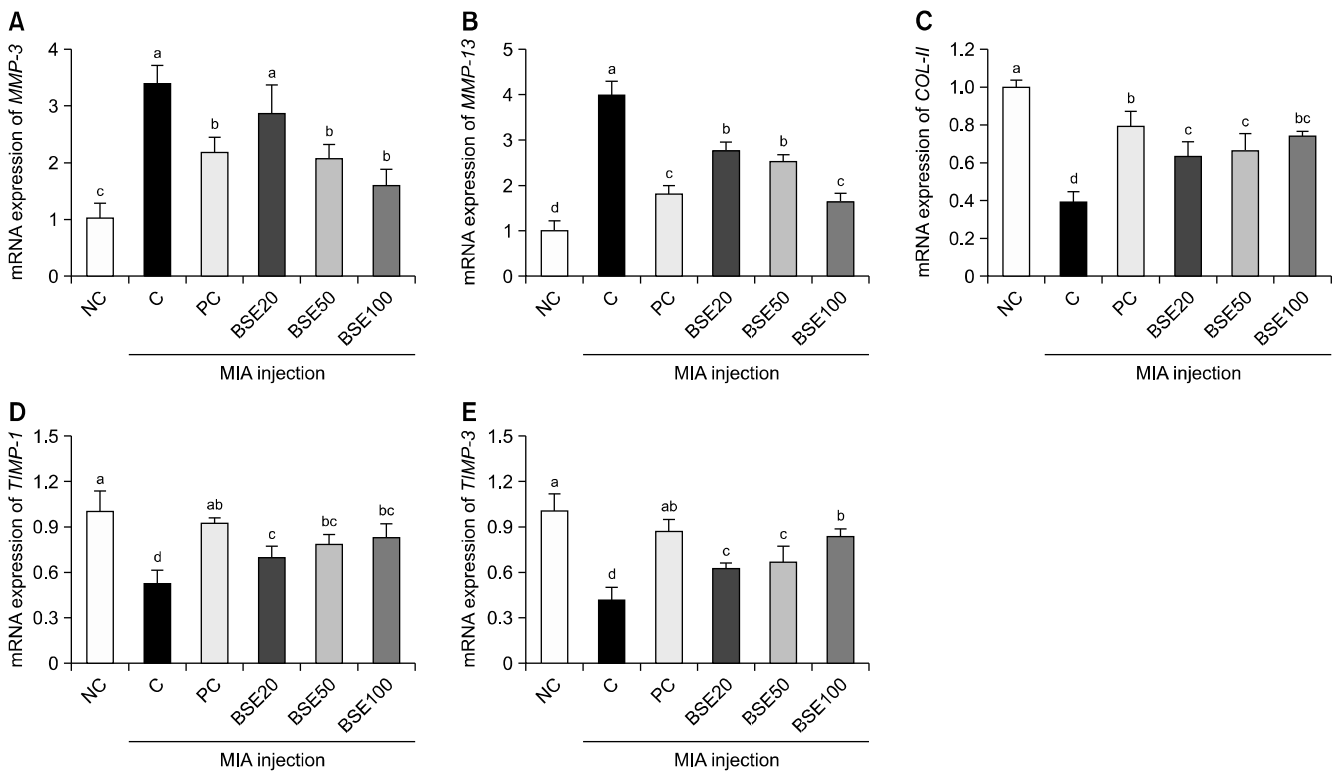


Fig. 3. The effect of *Boswellia serrata* extracts (BSE) on mRNA expressions of matrix metalloproteinase (MMP)-3 (A), MMP-13 (B), collagen type II (COL-1I, C), TIMP-1 (D), and TIMP-3 (E) of rats with monosodium iodoacetate (MIA)-induced osteoarthritis. Values are presented as mean \pm SD. Different letters (a-d) indicate a significant difference of $P < 0.05$, as determined using Duncan's multiple range test. NC, normal control group, AIN93G; C, control group, AIN93G+MIA injection; PC, positive control group, methylsulfonyl-methane (MSM) 300 mg/kg body weight (BW) in AIN93G+MIA injection; BSE20, BSE 20 mg/kg BW in AIN93G+MIA injection; BSE50, BSE 50 mg/kg BW in AIN93G+MIA injection; BSE100, BSE 100 mg/kg BW in AIN93G+MIA injection.

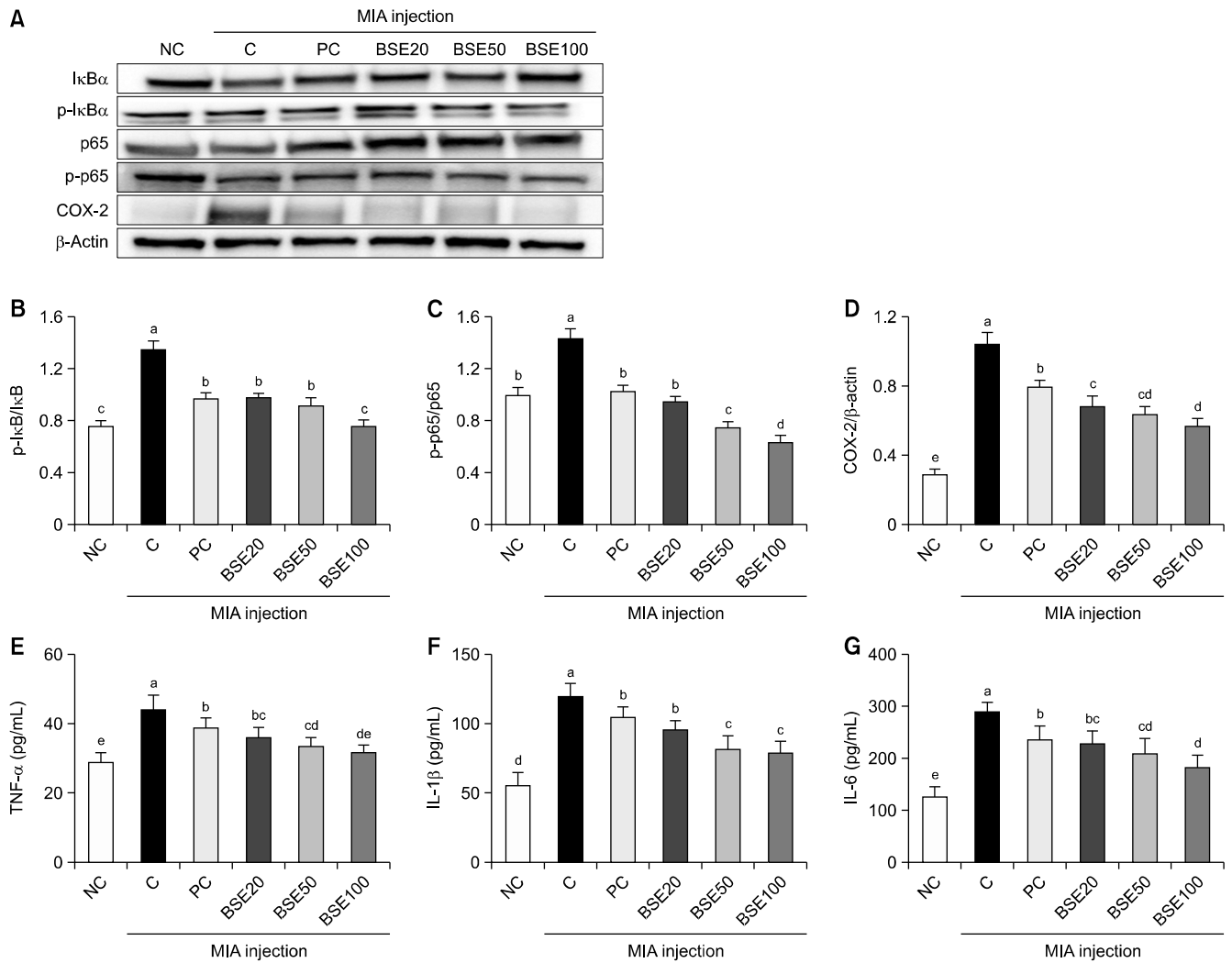


Fig. 4. The effect of *Boswellia serrata* extracts (BSE) on protein expressions (A, band image) of I κ B (B), nuclear factor κ B (NF- κ B, C), and COX-2 (D) and production of tumor necrosis factor (TNF)- α (E), interleukin (IL)-1 β (F), and IL-6 (G) of rats with monosodium iodoacetate (MIA)-induced osteoarthritis. Values are presented as mean \pm SD. Different letters (a-e) indicate a significant difference of $P < 0.05$, as determined using Duncan's multiple range test. NC, normal control group, AIN93G; C, control group, AIN93G+MIA injection; PC, positive control group, methylsulfonylmethane (MSM) 300 mg/kg body weight (BW) in AIN93G+MIA injection; BSE20, BSE 20 mg/kg BW in AIN93G+MIA injection; BSE50, BSE 50 mg/kg BW in AIN93G+MIA injection; BSE100, BSE 100 mg/kg BW in AIN93G+MIA injection.

of MMPs. These findings provide insights into the potential therapeutic actions of BSE in osteoarthritis.

FUNDING

None.

AUTHOR DISCLOSURE STATEMENT

The authors declare no conflict of interest.

AUTHOR CONTRIBUTIONS

Concept and design: Jinhak Kim, SE, Jinkyung Kim. Anal-

ysis and interpretation: all authors. Data collection: Jinhak Kim, SE. Writing the article: Jinhak Kim, Jinkyung Kim. Critical revision of the article: Jinkyung Kim. Final approval of the article: all authors. Statistical analysis: Jinhak Kim, Jinkyung Kim. Overall responsibility: Jinkyung Kim.

REFERENCES

- Akkiraju H, Nohe A. Role of chondrocytes in cartilage formation, progression of osteoarthritis and cartilage regeneration. *J Dev Biol.* 2015. 3:177-192.
- Ammon HP. Boswellic acids and their role in chronic inflammatory diseases. *Adv Exp Med Biol.* 2016. 928:291-327.
- Anderson DE, Johnstone B. Dynamic mechanical compression of chondrocytes for tissue engineering: a critical review. *Front Bioeng Biotechnol.* 2017. 5:76. <https://doi.org/10.3389/fbioe.2017.00076>
- Bonizzi G, Karin M. The two NF- κ B activation pathways and their

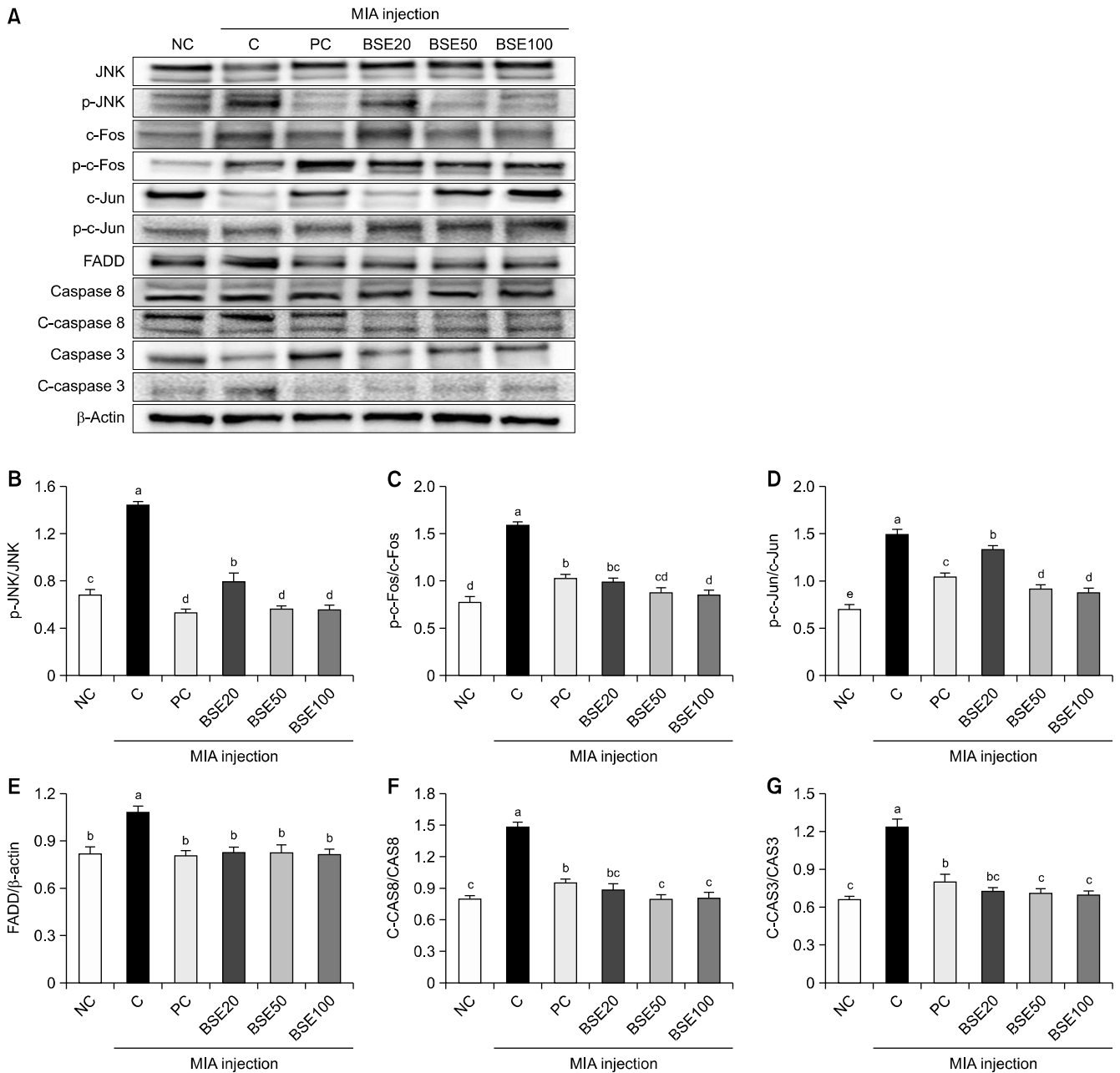


Fig. 5. The effect of *Boswellia serrata* extracts (BSE) on protein expressions (A, band image) of c-Jun N-terminal kinase (JNK, B), c-Fos (C), c-Jun (D), Fas-associated death domain protein (FADD, E), caspase 8 (F), and caspase 3 (G) of rats with monosodium iodoacetate (MIA)-induced osteoarthritis. Values are presented as mean \pm SD. Different letters (a-e) indicate a significant difference of $P < 0.05$, as determined using Duncan's multiple range test. NC, normal control group, AIN93G; C, control group, AIN93G+MIA injection; PC, positive control group, methylsulfonylmethane (MSM) 300 mg/kg body weight (BW) in AIN93G+MIA injection; BSE20, BSE 20 mg/kg BW in AIN93G+MIA injection; BSE50, BSE 50 mg/kg BW in AIN93G+MIA injection; BSE100, BSE 100 mg/kg BW in AIN93G+MIA injection.

role in innate and adaptive immunity. *Trends Immunol.* 2004. 25:280-288.

Grenier S, Bhargava MM, Torzilli PA. An *in vitro* model for the pathological degradation of articular cartilage in osteoarthritis. *J Biomech.* 2014. 47:645-652.

Hunter LJ, Wood DM, Dargan PI. The patterns of toxicity and management of acute nonsteroidal anti-inflammatory drug (NSAID) overdose. *Open Access Emerg Med.* 2011. 3:39-48.

Kashyap D, Garg VK, Goel N. Intrinsic and extrinsic pathways of apoptosis: role in cancer development and prognosis. *Adv Protein Chem Struct Biol.* 2021. 125:73-120.

Kim OK, Kim D, Lee M, Park SH, Jung J, Lee J. Krill oil attenuates

inflammation in monosodium iodoacetate-induced osteoarthritic rats, SW982 synovial cell line, and primary chondrocytes. *J Med Food.* 2022. 25:239-250.

Kizawa H, Kou I, Iida A, Sudo A, Miyamoto Y, Fukuda A, et al. An aspartic acid repeat polymorphism in asporin inhibits chondrogenesis and increases susceptibility to osteoarthritis. *Nat Genet.* 2005. 37:138-144.

Li MH, Xiao R, Li JB, Zhu Q. Regenerative approaches for cartilage repair in the treatment of osteoarthritis. *Osteoarthritis Cartilage.* 2017. 25:1577-1587.

Liu X, Machado GC, Eyles JP, Ravi V, Hunter DJ. Dietary supplements for treating osteoarthritis: a systematic review and meta-

- analysis. *Br J Sports Med.* 2018. 52:167-175.
- Lu S, Xiao X, Cheng M. Matrine inhibits IL-1 β -induced expression of matrix metalloproteinases by suppressing the activation of MAPK and NF- κ B in human chondrocytes *in vitro*. *Int J Clin Exp Pathol.* 2015. 8:4764-4772.
- Martin JA, Buckwalter JA. Roles of articular cartilage aging and chondrocyte senescence in the pathogenesis of osteoarthritis. *Iowa Orthop J.* 2001. 21:1-7.
- Nakatani K, Yamakuni T, Kondo N, Arakawa T, Oosawa K, Shimura S, et al. γ -Mangostin inhibits inhibitor- κ B kinase activity and decreases lipopolysaccharide-induced cyclooxygenase-2 gene expression in C6 rat glioma cells. *Mol Pharmacol.* 2004. 66:667-674.
- Rosenbaum CC, O'Mathúna DP, Chavez M, Shields K. Antioxidants and antiinflammatory dietary supplements for osteoarthritis and rheumatoid arthritis. *Altern Ther Health Med.* 2010. 16:32-40.
- Sarzi-Puttini P, Cimmino MA, Scarpa R, Caporali R, Parazzini F, Zaninelli A, et al. Osteoarthritis: an overview of the disease and its treatment strategies. *Semin Arthritis Rheum.* 2005. 35:1-10.
- Siddiqui MZ. *Boswellia serrata*, a potential antiinflammatory agent: an overview. *Indian J Pharm Sci.* 2011. 73:255-261.
- Wu CC, Bratton SB. Regulation of the intrinsic apoptosis pathway by reactive oxygen species. *Antioxid Redox Signal.* 2013. 19:546-558.